[1] This has been especially emphasized by K. Gottfried [CERN Report No. CERN TH 1735, 1973 (unpublished); Phys. Rev. Lett. 32, 957 (1974)]. See also A. Dar and J. Vary, Phys. Rev. D 6, 2412 (1972); P. M. Fishbane and J. S. Trefil, Phys. Rev. Lett. 31, 734 (1973); A. S. Goldhaber, Phys. Rev. D 7, 765 (1973).

[2] V. N. Gribov, Yad. Fiz. 9, 640 (1969) [Sov. J. Nucl. Phys. 9, 369 (1969)]. See also J. Kogut and L. Susskind, Phys. Rep. 8C, 78 (1973).

[3] In this paper the "bare" P is denoted by a dashed line and the physical P by a wavy line.

[4] V. N. Gribov and A. A. Migdal, Yad. Fiz. 8, 1002 (1968) [Sov. J. Nucl. Phys. 8, 583 (1969)].

[5] V. N. Gribov and A. A. Midgal, Zh. Eksp. Teor. Fiz. 55, 1498 (1968) [Sov. Phys.—JETP 28, 784 (1969)].

[6] V. A. Abramovskii, O. V. Kancheli, and V. N. Gribov, in Proceedings of the XVI International Conference on High Energy Physics, Chicago-Batavia, Ill., 1972, edited by J. D. Jackson and A. Roberts (NAL, Batavia, Ill., 1973), Vol. 1, p. 389.

[7] E. Lehman and G. A. Winbow, Daresbury Laboratory Report (in preparation).

[8] In a previous paper [E. Lehman and G. A. Winbow, Phys. Lett. 48B, 372 (1973)] we assumed on phenomenological grounds that centrally produced particles could cascade. This assumption is here shown to be wrong.

[9] J. Cardy and A. R. White, Nucl. Phys. B80, 12 (1974).

[10] J. B. Bronzan, Phys. Rev. D 7, 480 (1972).

[11] J. L. Cardy, Nucl. Phys. B79, 317 (1974).

[12] A. A. Migdal et al., Phys. Lett. 48B, 239 (1974).

[13] R. J. Glauber, in High Energy Physics and Nuclear Structure, edited by G. Alexander (North-Holland, Amsterdam, 1967), p. 311.

[14] J. V. Allaby et al., Yad. Fiz. 12, 538 (1970) [Sov. J. Nucl. Phys. 12, 295 (1971)].

[15] B. W. Allardyce et al., Nucl. Phys. A209, 1 (1973).

[16] M. Gell-Mann and B. M. Udgaonkar, Phys. Rev. Lett. 8, 346 (1962).

[17] H. D. I. Abarbanel and J. B. Bronzan, Phys. Rev. D 9, 2397 (1974).

[18] H. D. I. Abarbanel and J. B. Bronzan, Phys. Rev. D 9, 3304 (1974).

[19] M. I. Atanelishvili et al., Zh. Eksp. Teor. Fiz. Pis'ma Red. 18, 490 (1973) [JETP Lett. 18, 288 (1974)].

[20] V. V. Ammosov et al., Nucl. Phys. B58, 77 (1973).

[21] Many of the data are discussed and summarized in Ref. 1. See also J. Gierula and W. Wolter, Acta Phys. Pol. B2, 95 (1971), and E. L. Feinberg, Phys. Rep. 5C, 240 (1972), for general discussions of cosmic-ray results.

[22] Barcelona-Batavia-Belgrade-Bucharest-Lund-Lyons-Montreal-Nancy-Ottawa-Paris-Rome-Strasbourg-Valencia Collaboration (J. Hébert et al.), Phys. Lett. 48B, 467 (1974).

[23] E. M. Friedlander et al., Nuovo Cimento Lett. 9, 341 (1974). These data differ from those of J. Babecki et al., Phys. Lett. 47B, 268 (1973).

[24] L. D. Landau, Izv. Akad. Nauk SSSR 17, 51 (1953); S. Z. Belen'kij and L. D. Landau, Nuovo Cimento Suppl. 3, 15 (1956).

[25] I. Ya. Pomeranchuk, Dokl. Akad. Nauk SSSR 78, 889 (1951).

[26] K. M. Abdo et al., Dubna Report No. DUBNA E1-7548 1973 (unpublished).

[27] O. V. Kancheli, Zh. Eksp. Teor. Fiz. Pis'ma Red. 18, 465 (1973) [JETP Lett. 18, 274 (1973)].

Unified description of inclusive and exclusive reactions at all momentum transfers*

R. Blankenbecler and S. J. Brodsky

Stanford Linear Accelerator Center, Stanford University, Stanford, California 94305
(Received 28 May 1974)

The constituent-interchange model is used to relate large- and small-momentum-transfer reactions, to relate inclusive and exclusive processes, and to predict the form of the inclusive cross section throughout the Peyrou plot. Two important corrections to the triple-Regge formula are derived. The first, important at a small missing mass, allows a smooth connection to exclusive processes. The second, important at large missing mass, allows a smooth connection to the central region and to the large-transverse-momentum regime. Simple quark-counting rules are given which predict the limiting behavior of Regge trajectories and residue functions, and also the powers of P_T^2 and the missing-mass dependence of inclusive cross sections. Many experimental consequences of the model are given.

I. INTRODUCTION

One of the most exciting aspects of large-transverse-momentum hadron reactions is the possibility that we can probe the simplest constituent structure and underlying dynamics of hadronic matter at short distances. Recent data for inclusive and exclusive processes at large p_T appear to be consistent with scaling laws of the form[1-4]

$$E\frac{d\sigma}{d^3p}(A+B\to C+X)\to(p_T^2)^{-N}f\left(\frac{\mathfrak{M}^2}{s},\frac{t}{s}\right)$$

and[5,6]

$$\frac{d\sigma}{dt}(A+B\to C+D)\to(p_T^2)^{-N}f\left(\frac{t}{s}\right)$$

from $p_{lab} = 5$ to 2000 GeV/c, and have given support to field-theoretic composite-hadrons models[7−13] with the degrees of freedom of the quark model. In the case of exclusive processes, the observed power-law behavior in p_T is consistent with the simple dimensional-counting prediction $N = n - 2$, where n is the total minimum number of elementary fields in the external particles, A, B, C, and D.[14] The angular distributions of the exclusive processes $f(t/s)$ are also consistent[9] with the hypothesis of the constituent-interchange model (CIM) that the important elementary interaction between hadrons is the interchange and exchange of common quark constituents; hard-gluon exchange between quarks of different hadrons does appear to be suppressed at large p_T.[15]

In the case of the inclusive processes at large p_T, the predicted power from dimensional counting is $N = n - 2$, where n is the minimum number of fields required in the elementary irreducible subprocess responsible for the production of C at large transverse momentum. In the CIM, the minimum subprocesses involve quark-hadron scattering and have $n \geq 6$, or $N \geq 4$. Again, this seems to be consistent with the recent measurements at the CERN Intersecting Storage Rings (ISR)[1] and Fermi National Accelerator Laboratory (FNAL).[2] A rough analysis of the reactions $pp \to \pi X$ and $pp \to pX$ are consistent with values of $2N$ ranging from 8 to 12. Therefore scale-invariant quark-quark gluon-exchange interactions ($N = 2$) are apparently absent, or at least not required by the data.

In contrast to the possible theoretical simplicity of large-p_T reactions, the physics of small-t and -u processes are complicated by the coherent multiparticle and multiperipheral nature of Regge behavior. Nevertheless, as emphasized by Bjorken and Kogut[16] and demonstrated explicitly in Refs. 8 and 17, there must be a continuity of dynamics from large to small momentum transfers. By assuming a smooth connection between these two domains, one obtains conditions on the normalization and functional dependence of the large-transverse-momentum reactions in direct analogy with the Drell-Yan[18] relation and Bloom-Gilman duality[19] for electroproduction.

In this paper we turn the "correspondence" argument around and investigate the implications and constraints on low-momentum phenomena in order that the physics in the Regge region is consistent with power-law scaling behavior at large transverse momentum. We emphasize here one feature of the CIM which is different from other parton models: Once the basic irreducible amplitude is given, the calculation proceeds by using only hadron intermediate states in order to produce the

full complexities of Regge behavior in the amplitude.

This paper thus represents an attempt toward the theoretical unification of the underlying physics of the many kinematic domains of inclusive and exclusive processes (see Fig. 1). We shall attempt to clarify the relations between large- and small-momentum-transfer reactions, to explore the exclusive-inclusive connection, and to predict the limiting forms of the inclusive cross section at the kinematic boundaries. Among our new results are the following:

(1) The domain of applicability of the simplest Regge formulas for inclusive reactions is more limited than usually supposed. The usual triple-Regge formula,[20] because of the restriction $\mathfrak{M}^2 \gg |t|$, cannot be continued into the resonance region or exclusive limit. However, we shall present a cross section R_r valid for small $\mathfrak{M}^2/s$ which connects smoothly onto (i) the large-transverse-momentum region, (ii) the exclusive and resonance region at any $\theta_{c.m.}$, and (iii) the triple-Regge formula for the fragmentation region $s \gg \mathfrak{M}^2 \gg t$. The formula for R_r respects the CIM and the dimensional-counting rules at large momentum transfer and obeys a generalized Drell-Yan−Bloom-Gilman duality at the exclusive limit.

(2) The consistency of Regge behavior and power-law falloff at large transverse momentum demands that the effective trajectory $\alpha_{AC}(t)$, which appears in exclusive reactions and the triple-Regge formulas for inclusive cross sections, approach negative integers as $t \to -\infty$. We present an extended dimensional-counting formula for $\alpha_{AC}(-\infty)$ for all A and C including exotic channels in Sec. II B.

(3) Throughout most of the allowed kinematic domain of inclusive reaction, i.e., for finite $\mathfrak{M}^2/s$, fragmentation (hadronic bremsstrahlung) will occur from both target and beam projectiles. In Sec. IV we present a cross section R_c for the entire interior or central region of the Peyrou plot which is expressed in terms of a convolution of R_r contributions. In this case, we find that R_c connects smoothly to the central Regge region [$s \to \infty$, t, and $u \lesssim O(\sqrt{s})$], and yields a generalized multiperipheral type of description of low-p_T processes. On the other hand, we find that R_c may play a critical, unexpectedly important role in the triple-Regge domain. These new important contributions, which originate (for $t/s \to 0$) from beam fragmentation and dissociation diagrams, correspond to disconnected cut contributions and cannot be identified with a simple Regge singularity of an exclusive process. The analogous contributions in inelastic Compton scattering and photoproduction yield important background terms at large transverse momentum

and small $\mathfrak{M}^2/s$.

We thus find that examining the inclusive cross section from the perspective of the entire kinematic domain of both large and small momentum transfer leads to many unexpected relationships. The formulas for R_r and R_c serve as a link between the normally separated domains of inclusive reactions. Most satisfactorily, the underlying quark constituent structure which yields power-law behavior is only evident at large p_T; our description melds into a purely hadronic-state analysis at small momentum transfers.

In addition to determining the power-law behavior and effective trajectories $\alpha_{AC}(t)$ at large transverse momentum, we can extend dimensional counting to completely determine the threshold dependence ($\mathfrak{M}^2/s \to 0$) of the inclusive cross section at any angle, including $t = 0$. First, some definitions are needed.

We shall describe the most general scattering processes which contribute to $A + B \to C + X$ according to the classification shown in Fig. 2. The subprocess $a + b \to C + d^*$ which produces the detected particle is by definition *hadron-irreducible* in that neither a nor b fragments (i.e., emits hadronic bremsstrahlung before interaction). We define the probability of finding the irreducible state a in the incident hadron A with fractional longitudinal momentum x (in the infinite momentum frame of A) as $G_{a/A}(x)$. Dimensional counting then gives for $x \sim 1$ (see Sec. IIA),

$$G_{a/A}(x) \sim (1 - x)^{g(a/A)} \ ,$$

where

$$g(a/A) = 2n(\bar{a}A) - 1 \ .$$

Here $n(\bar{a}A)$ is the minimum number of quark fields in the state $\bar{a}A$. [For $a = A$, i.e., no beam fragmentation, we can formally take $g = -1$.] We find that the subprocess $a + b \to C + d^*$ then gives a contribution of the form [$\mathfrak{M}^2/s \sim 0$, $x_L = p_L^{c.m.}/p_L^{max} > 0$]

$$E \frac{d\sigma}{d^3p} \sim f_{ab \to Cd^*}(p_T^2) \left(\frac{\mathfrak{M}^2}{s}\right)^{g(a/A)+g(b/B)+1}$$

$$\times \left(\frac{p_T^2}{s} + \bar{y}\frac{\mathfrak{M}^2}{s}\right)^{1-g(b/B)-2\bar{\alpha}_{ac}} \ , \tag{1}$$

where $f(p_T^2) \sim (p_T^2)^{2-n_a-n_b-n_C-n_d*}$ for large p_T and $\bar{y} \sim [g(b/B)+1]/[g(a/A)+g(b/B)+2]$. The threshold dependence can be critically angular-dependent. Thus in the forward direction ($p_T^2/s \to 0$, $x_L \to 1$) we have the threshold behavior

$$E \frac{d\sigma}{d^3p} \sim (1 - x_L)^{g(a/A)+2-2\bar{\alpha}_{ac}} \ , \tag{2}$$

where $\bar{\alpha}_{aC} \simeq \alpha_{aC}(x_L t)$ is the effective trajectory coupling a to C. This agrees with the usual triple-

Regge formula if A does not fragment [$g(a/A) = -1$]. However, in most cases, especially for exotic channels, fragmentation of the beam will be an important contribution for finite $\mathfrak{M}^2/s$ values. In particular, if we consider the diffractive subprocess $C + b \to C + b$, then $\bar{\alpha}_{CC} \to 1$ at $t \to 0$, and we obtain the direct dissociation term

$$E \frac{d\sigma}{d^3p} \sim (1 - x_L)^{g(C/A)} = (1 - x_L)^{2n(\bar{C}A)-1} \quad (t \sim 0) \ ,$$

in place of the triple-Regge term $(1 - x_L)^{1-2\alpha_{AC}(0)}$. This gives an "effective" trajectory

$$\alpha_{AC}^{eff} = \tfrac{1}{2}[1 - g(C/A)]$$

$$= 1 - n(\bar{C}A) \ . \tag{3}$$

Again we emphasize that this contribution falls outside the scope of the usual triple-Regge analysis since it derives from beam fragmentation and is usually associated with the central (or double-Regge) region. The definiteness of the CIM allows one to continue these contributions into the triple-Regge region. The comparison of these predictions with experiment is given in Sec. V.

At large transverse momentum, the threshold dependence of Eq. (1) for the subprocesses $(a + b \to C + d^*)$ is $(\mathfrak{M}^2/s)^{g(a/A)+g(b/B)+1}$. This behavior, together with the predicted power-law dependence in p_T^2, and the distinctive quantum-number character, multiplicities, and correlations of the final states, allows an unraveling of the contributions of the various subprocesses $a + b \to C + d^*$ which can contribute in different kinematic domains of the inclusive cross section. This will be discussed further in Sec. II B, and the leading subprocesses are summarized in Table I.

The organization of this paper is as follows: In Sec. II we present a useful decomposition of the inclusive cross section which separates the complications of hadronic bremsstrahlung (fragmentation) from the basic hadron-irreducible scattering subprocess. The properties of the hadronic structure function $G_{a/A}(x)$ are reviewed and the threshold dependence at $x \to 1$ is computed using dimensional counting. The computation of the irreducible subprocess in the CIM is then presented. We also give a new, general, dimensional-counting formula for the asymptotic trajectory $\alpha_{AC}(-\infty)$ coupling any two hadron states A and C, and the corresponding residue functions.

In Sec. III we present an analysis of the exclusive-inclusive connection and a generalization of the triple-Regge formula. The complete cross section, allowing for both beam and target fragmentation, is then computed in Sec. IV, and the threshold dependence at the various kinematic boundaries is made explicit. Additional applications are dis-

cussed in Sec. V. A section with a discussion and conclusion then follows.

II. DECOMPOSITION OF THE INCLUSIVE CROSS SECTION

The entire kinematic range of high-energy inclusive reactions is illustrated on the Peyrou plot of Fig. 1. As usual we define

$$s = (p_A + p_B)^2, \quad t = (p_A - p_C)^2,$$

$$u = (p_B - p_C)^2, \quad \mathfrak{M}^2 = (p_A + p_B - p_C)^2,$$

and

$$\epsilon = \mathfrak{M}^2/s \cong (1 - p_{c.m.}/p_{max}),$$

$$x_T = p_T/p_{max}, \quad x_L = p_L/p_{max} \cong (t-u)/s.$$

The resonance region and exclusive scattering limit occur near or at the kinematic boundary on the circle. The position of the triple-Regge region is shown schematically, as is the central region.

The decomposition of the inclusive scattering process displayed in Fig. 2 is extremely useful for separating the effects of peripheral interactions and hadronic bremsstrahlung (or fragmentation) from the effects due to basic elementary processes dependent upon constituent structure. The subprocess $a + b \to C + d^*$ is *hadron-irreducible* in that neither hadron a nor hadron b can produce another hadron by the bremsstrahlung process before interacting (see Fig. 3). Using this decomposition, we can compute the total inclusive cross section as

$$E \frac{d\sigma}{d^3p} (A + B \to C + X)$$

$$= \sum_{a,b} \int_0^1 dx_a \int_0^1 dx_b \, G_{a/A}(x_a) \, G_{b/B}(x_b)$$

$$\times \frac{d\sigma^I}{d^3p/E} (a + b \to C + d^*) . \quad (4)$$

The superscript I means hadron-irreducible, and the basic irreducible subprocess $a + b \to C + d^*$ is evaluated at

$$s' = (p_a + p_b)^2 \cong x_a x_b s,$$

$$t' = (p_a - p_c)^2 \cong x_a t,$$

$$u' = (p_b - p_c)^2 \cong x_b u,$$

$$p_T'^2 = \frac{tu}{s} = p_T^2.$$

The missing-mass state X in general consists of beam fragments $(X\bar{a})$, target fragments $(X\bar{b})$, and the system (d^*) which is produced in the basic irreducible subprocess and carries the balancing
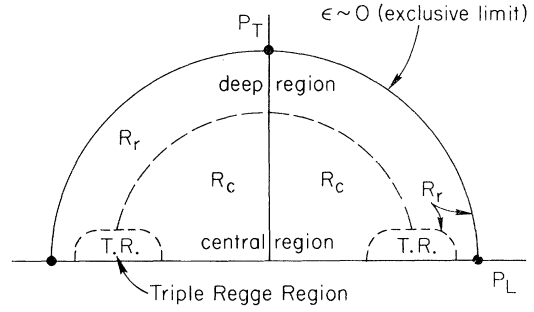

FIG. 1. Schematic representation of the various kinematical domains within the Peyrou plot for the inclusive reactions $A + B \to C + X$. The cross section R_r discussed in Sec. III connects smoothly onto the triple-Regge formula for inclusive reactions and the exclusive cross sections in both the fixed-t Regge limit and the fixed-angle deep scattering region. The cross section R_c, discussed in Sec. IV, should dominate the interior central region of large missing mass.

transverse momentum.

Note that it is also possible to compute the average missing mass of the state d^* directly from $(\mathfrak{M}_{d^*}^2 = s' + t' + u')$

$$E \frac{d\sigma}{d^3p} (A + B \to C + X) \langle \mathfrak{M}_{d^*}^2 \rangle$$

$$= \sum_{a,b} \int_0^1 dx_a \int_0^1 dx_b \, G_{a/A}(x_a) \, G_{b/B}(x_b) (s' + t' + u')$$

$$\times \frac{d\sigma^I}{d^3p/E} (a + b \to C + d^*) .$$

In general, one has

$$\langle \mathfrak{M}_{d^*}^2 \rangle = p_T^2 f(\epsilon, x_T^2) ,$$

where $f(\epsilon, 0)$ does not vanish, and f decreases as $\epsilon \to 0$. This allows an estimate of the associated multiplicity (if the entire recoiling system is detected) if one assumes that the multiplicity of d^* is linear in $\ln \langle \mathfrak{M}_{d^*}^2 \rangle$, as in typical hadronic events.

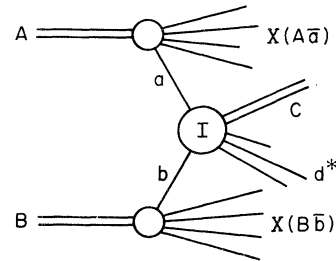The function $G_{H/A}(z)$ gives the probability that a

FIG. 2. The general decomposition of inclusive reactions. The overall inclusive process $A + B \to C + X$ is written as a sum of hadron-irreducible processes $a + b \to C + d^*$.

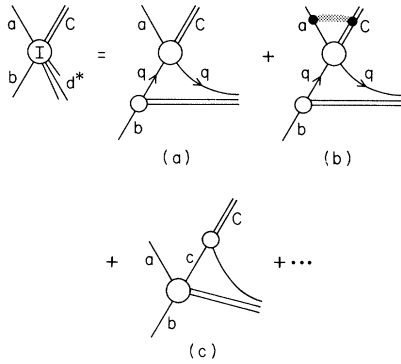FIG. 3. The interior structure of the irreducible sub-process $a+b \to C+d*$.

hadron A with infinite momentum will emit a hadron H with fractional longitudinal momentum z ($0 < z < 1$), as has been discussed in Ref. 8 and Sec. I. Note that the convolution formula (4) neglects the transverse-momentum distribution and certain off-shell effects in intermediate states. These corrections will be inessential in the applications discussed here.

The summation in Eq. (4) implicitly includes the direct contributions to the inclusive cross section where fragmentation from the target B and/or the projectile A does not occur. In this case, one clearly has $G_{H/A}(z) \propto \delta(1-z)$. In general, fragmentation from the initial particles is only suppressed when we approach the exclusive limit $\mathfrak{M}^2/s \to 0$. The nature of this suppression, however, depends critically on the production angle. For processes at large transverse momentum with $4p_T^2/s$ approaching 1, a finite fraction of the momentum of both A and B is required in the basic production subprocess, and bremsstrahlung from both incident particles will be kinematically suppressed. This is the deep region of inclusive scattering which is most sensitive to short-distance effects and which will smoothly connect onto large-angle exclusive scattering.

On the other hand, at small momentum transfers ($p_T^2 = tu/s \sim 0$) in the forward direction, hadronic bremsstrahlung from just the projectile A will be suppressed as we approach the exclusive limit ($1 - x_L \sim \mathfrak{M}^2/s \to 0$); however, fragmentation from the target is allowed. This is the triple-Regge (or fragmentation) region which is usually described in terms of the Regge poles $\alpha_{AC}(t)$ in the $\overline{A}C$ channel observed in elastic scattering.

More generally, we shall divide the Peyrou plot of Fig. 1 into a central region (which includes the central Regge region, roughly $|x_L| \lesssim \frac{1}{2}$ at small momentum transfer) and an outer ring region. In the outer region, which is described by the cross section R_r (see Sec. III), hadronic bremsstrahlung

from at least one hadron is suppressed. In the central region, which will be described by the reducible cross section R_c (see Sec. IV), bremsstrahlung from A and B has no strong suppression and must be included.

A. The properties of the distribution functions $G_{H/A}(z)$

In order to describe the reducible contributions to the inclusive cross section we shall require the properties of the hadronic distribution functions $G_{H/A}(z)$. In particular, the central Regge region is sensitive to the small-z behavior of both $G_{a/A}$ and $G_{b/B}$. On the other hand, the $\epsilon \to 0$ dependence requires the $z \to 1$ behavior of either or both distribution functions. In fact, we shall show that all of the essential features of the $G(z)$ can be predicted, and thus these are not functions to be fitted to experiment, but will serve as critical tests of the model.

By momentum conservation, we have

$$\sum_H \int_0^1 dz\, z\, G_{H/A}(z) = 1 \,, \qquad (5)$$

which serves as an overall normalization constraint. The distribution function for quark-partons in hadron A can clearly be written as a convolution:

$$G_{q/A}(x) = \int_x^1 \frac{dz}{z} \sum_H G_{q/H}^I(x/z)\, G_{H/A}(z) \,, \qquad (6)$$

where the summation is over all irreducible hadron states H which contain a quark of type q. The deep-inelastic structure function is given by the familiar relation

$$F_{2H}(x) = x \sum_q \lambda_q^2 G_{q/A}(x) \,,$$

where λ_q is the quark charge. The notation $G_{q/H}^I$ in Eq. (6) denotes that it originates directly from a hadron-irreducible wave function—computed without hadron intermediate states. As discussed in Ref. 16 the Bethe-Salpeter wave function of the irreducible hadron H has asymptotic power-law behavior and is responsible for the power-law falloff of exclusive scattering amplitudes at fixed angle, form factors, and the Drell-Yan-West relation.[18]

For $x \to 1$, the threshold power $g(q/A)$ can be introduced as

$$G_{q/A}(x) \sim G_{q/A}^I(x) \sim (1-x)^{g(q/A)} \,.$$

Dimensional counting then gives the result

$$g(q/A) = 2N - 1 \,, \qquad (7)$$

where N is the minimum number of left-over quarks that are necessary for hadron A to produce

the quark of type q. Now using Eq. (6), one easily sees that the only consistent threshold dependence of $G_{H/A}$ is given by

$$G_{H/A}(x) \sim (1-x)^{g(H/A)} \quad (x \to 1) \, ,$$

and (8)

$$g(H/A) = 2n(\bar{H}A) - 1 \, ,$$

where $n(\bar{H}A)$ is the minimum number of quarks that can be produced in the process $A + \bar{H} \to$ quarks.

This simple yet interesting result only depends on constituent counting and the assumption of an underlying scale-invariant hadronic theory on the quark level. Sample values of $g(H/A)$ are easily computed with the above rule: $g(p/p) = -1$ [this actually represents $G_{p/p} \propto \delta(1-z)$] or 3, $g(\pi^{\pm}/p) = 5$, $g(K^+/p) = 5$, $g(K^-p) = 9$, $g(\bar{p}/p) = 11$, and $g(\pi/\rho) = 3$. Note also $g(q/p) = 3$, $g(\bar{q}/p) = 7$ for antiquarks and strange quarks in the nucleon, and $g(q/\pi) = 1$. Some of these latter results have also been independently derived (in a different manner) by Farrar,[21] and Gunion[22] has given a derivation of all these numbers using infinite-momentum-frame techniques.

It has been shown in Ref. 16 that the small-z behavior of $G_{H/A}$ is determined by the leading Regge trajectory in the $\bar{A}A \to \bar{H}H$ channel, i.e., the leading behavior of $\sigma_{\bar{A}H} \sim s^{\alpha_A(0)-1}$. A form of $G_{H/A}$ that has the correct behavior as $z \sim 0$ and $z \sim 1$ is

$$G_{H/A}(z) = z^{-\alpha_A(0)}(1-z)^{g(H/A)} \, . \quad (9)$$

This simple behavior will be used throughout this paper, but it could be multiplied by any smooth function of z without modifying any of our essential results.

Using Eq. (6), the deep-inelastic structure function has the form

$$F_{2B}(x) = \int_x^1 dz \sum_H F_{2H}^I(x/z) G_{H/B}(z) \, , \quad (10)$$

where F_{2H}^I is the hadron-irreducible structure function. This equation is illustrated in Fig. 4. Note, as has been emphasized in Ref. 17, that the Regge behavior of $G_{H/B}(z)$, which in turn reflects the hadronic bremsstrahlung of the target particle B, leads to Regge behavior for the structure function at small x.

B. The structure of the irreducible subprocess

The most critical physics of an inclusive reaction occurs in the irreducible subprocess $a + b \to C + d^*$ and in a certain sense, this is physically the most interesting object to study. The major complication of inclusive processes—hadronic radiation from the incident particle—is, by definition, removed.

At small momentum transfer, the irreducible subprocess amplitude has the conventional ex-
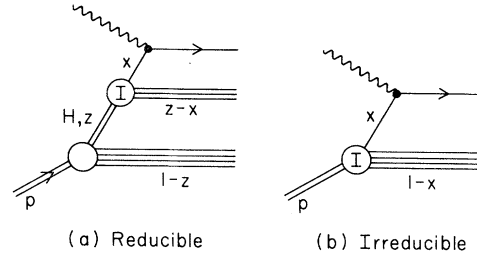

(a) Reducible (b) Irreducible

FIG. 4. The decomposition of the structure function $\nu W_{2p}(x)$ into its hadron-reducible and hadron-irreducible components.

pansion in terms of Regge trajectories $\alpha_{ac}(t)$ for $t \sim 0$ and $\alpha_{bc}(u)$ for $u \sim 0$, where α_{ac} and α_{bc} are the same trajectories that occur in exclusive processes. This is *not* always true for the reducible contributions, as emphasized in Sec. IV. At high momentum transfer, the subprocess occurs at an energy

$$s_{ab} \gtrsim 4p_T^2 \, .$$

It is therefore sensitive to the same short-distance effects which occur in high-energy fixed-angle exclusive scattering. In the large-momentum-transfer region we will use the constituent-interchange model developed in Refs. 8, 9, and 17, which has a wide range of experimental support. This support ranges from 5-GeV/c exclusive experiments at fixed angle to the large-transverse-momentum exclusive experiments at NAL and the CERN ISR.

The main hypothesis of the interchange model is that only quark-hadron interactions are important at short distances; direct interactions between quarks of different hadrons are assumed to be negligible. Exclusive scattering of hadrons at fixed angle is thus accounted for by the exchange or interchange of common quarks between the hadrons.

By using dimensional counting and a specific choice of quantum numbers for the constituents, we can completely specify the asymptotic behavior of the irreducible CIM amplitude. At fixed angles, the exclusive amplitude M for $A + B \to C + D$ scales as

$$M \sim s^{(4-n_A-n_B-n_C-n_D)/2} f(\theta_{c.m.}) \, , \quad (11)$$

where n_A is the number of elementary fields in A, etc. The amplitude can also be written in Regge form as

$$M \sim \beta_{BD}(t)(-u)^{\alpha_{AC}(t)} + \bar{\beta}_{BD}(t)(-s)^{\alpha_{AC}(t)}$$
$$+ \cdots$$

for fixed t, $s \to \infty$. The asymptotic behavior of the trajectory α_{AC} at large t is controlled by the quark-hadron scattering amplitude as in Fig. 5, and the

ratio of the residues is determined by the quantum numbers of the constituents. It is now easy to see that for $t \to -\infty$ one has [these results are extensions of the formula given in Ref. 14, and we assume for $s \gg t$ that $M(qA \to qC)$ depends only on s and u]

$$\alpha_{AC}(-\infty) = \tfrac{1}{2}(4 - n_A - n_C - n_{\text{int}}) \qquad (12)$$

and

$$\beta_{BD}(t), \ \bar{\beta}_{BD}(t) \sim (-t)^{(n_{\text{int}} - n_B - n_D)/2}, \qquad (13)$$

where n_{int} is the minimum number of exchanged quarks compatible with the external states. The necessary cancellations between trajectories that are required for the factorization of residues are derived and discussed in Ref. 17. Only the dominant diagrams were kept in the above derivation.

Some representative asymptotic trajectories $\alpha_{AC}(t \to -\infty)$ using quark counting are as follows.

$\alpha_{\pi\pi}(-\infty) = \alpha_{KK}(-\infty) = -1$	Pomeron, ρ, ω, ϕ, etc.
$\alpha_{pp}(-\infty) = \alpha_{pn}(-\infty) = -2$	Pomeron, ρ, ω, ϕ, etc.
$\alpha_{\pi p}(-\infty) = -2$	N, Δ
$\alpha_{K^+ p}(-\infty) = -2$	Λ, Σ
$\alpha_{K^- \pi^-}(-\infty) = -1$	K^*
$\alpha_{\pi^+ K^-}(-\infty) = \alpha_{\pi^+ \pi^-}(-\infty) = -2$	exotic
$\alpha_{K^- p}(-\infty) = -3$	exotic
$\alpha_{p\bar{p}}(-\infty) = \alpha_{p\bar{n}}(-\infty) = -4$	exotic

These results are in agreement with pp and $\pi^- p$ elastic scattering.[23, 24]

We also can predict the limits of the resultant effective trajectories induced by the pointlike aspect of the photon ($n_\gamma = 1$):

$$\alpha_{\gamma\gamma}(-\infty) = 0 \quad (J = 0 \text{ fixed pole}) ,$$

$$\alpha_{\gamma\pi}(-\infty) = -\tfrac{1}{2} ,$$

$$\alpha_{\gamma p}(-\infty) = -\tfrac{3}{2}$$

(although spin may modify these last two results). Also, for the case of inclusive processes at large transverse momentum, we need the values
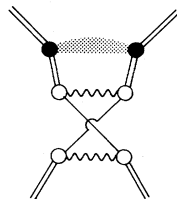

FIG. 5. The virtual hadronic bremsstrahlung, which gives rise to full Regge behavior in the CIM.

$$\alpha_{q\pi}(-\infty) = 0$$

and

$$\alpha_{qp}(-\infty) = -1 .$$

In general, the signature and possible exchange-degeneracy of the trajectories are controlled by the assumed types of quarks which can be exchanged in the t channel. Notice that exotic as well as ordinary trajectories are specified by the CIM at $t \to -\infty$. The iteration of the basic CIM irreducible kernel in the t channel will produce a moving trajectory, which then connects with normal Regge phenomenology at $t \sim 0$ and eventually connects to the particle bound states in the $\bar{A}C$ channel at positive t. Accordingly, it is natural to expect that the exotic trajectories remain quite near to their asymptotic $t \to -\infty$ values and even at $t = 0$ may not be very high above this value.

The basic irreducible subprocesses of the CIM for inclusive processes are shown in Fig. 3. In Fig. 3(a) an irreducible hadron state a of the projectile interacts (via constituent interchange) with a quark state of hadron B. We can compute the quark probability function $G_{q/B}$ via hadron-irreducible intermediate hadron state b, as in Eq. (6), or directly via Eq. (9). The quark-hadron scattering amplitude $a + q \to C + q$ in Fig. 3(a) yields, for deep-inelastic hadron scattering, an "effective current" which is the analogue of the $e + q \to e' + q$ amplitude in deep-inelastic lepton scattering. We thus have immediately

$$\frac{d\sigma}{dt\,dx}(a + B \to C + x)$$

$$= \sum_q G_{q/B}(x) \frac{d\sigma}{dt}(a + q \to C + q)\Big|_{\substack{s'=xs \\ t'=t}}, \quad (14)$$

where $x = -t/(\mathfrak{M}^2 - t) = -t/(s + u)$ is Bjorken's scaling variable and

$$E \frac{d\sigma}{d^3p} = \frac{sx}{\pi(s+u)} \frac{d\sigma}{dt\,dx} .$$

We emphasize that we have automatically included fragmentation from the target particle B by using the structure function $G_{q/B}(x) \propto F_{2B}(x)/x$. Then by convolution with $G_{a/A}(z)$ and summation over the irreducible states a we obtain the full cross section for $A + B \to C + D$. Note that, formally, Eq. (4) can now be applied both when a and b are hadron-irreducible states with hadronic quantum numbers and also at the short-distance level where a and/or b can be taken as a hadron-irreducible quark-parton state.

Clearly in the exclusive limit where $\epsilon \to 0$, we will obtain the analogue of the Drell-Yan relation and Bloom-Gilman duality, i.e., we shall obtain a smooth connection between the inclusive reaction

$H + B \rightarrow C + X$ (where H is a hadron-irreducible) and exclusive channels $H + B \rightarrow C + D$ (calculated via the CIM at the corresponding t). This will be discussed in detail in Sec. III.

As t becomes small, the "virtual" hadron bremsstrahlung diagrams [Fig. 4(b)], where hadrons are emitted by a and are absorbed by C, become important and build up normal Regge trajectories $\alpha_{aC}(t)$.

In this way, the internal quark description, which is required in order to understand the power-law behavior and angular structure of reactions at large transverse momentum melds into the conventional hadronic description at small momentum transfer. This effect, along with the exclusive-inclusive connection, extends the validity of the correspondence principle proposed by Bjorken and Kogut.[16]

Another potentially important contribution to the irreducible subprocess at large transverse momentum is the "fusion" process, which has been particularly emphasized by Landshoff and Polkinghorne.[10] The important fusion processes are evidently $q + \bar{q} \rightarrow$ meson + meson*, and $q + q \rightarrow$ baryon + $\bar{q}$. In the first case, assuming C is a meson, we compute

$$\frac{d\sigma}{dt\,dx}(q + B \rightarrow C + X) = G_{\bar{q}/B}(x)\,\frac{d\sigma}{dt}\,(q + \bar{q} \rightarrow C + \overline{C}*)\Big|_{\substack{s'=xs \\ t'=t}},$$

(15)

and then convolute with $G_{q/A}$ as in Eq. (4) to obtain the full inclusive reaction $A + B \rightarrow C + X$.

In addition to quark interchange and fusion, we can also have "reverse fusion" based on the process $M + \overline{M} \rightarrow q + \bar{q}$. The detected hadron C is then emitted along the quark-jet direction, with probability given by the quark fragmentation $G_{q/C}$ as discussed by Berman, Bjorken, and Kogut.[7] In this case the final state contains two jets, and should be analogous to the final state produced in

TABLE I. The expected dominant subprocesses for selected hadronic inclusive reactions at large transverse momentum. The second column lists the important exclusive processes which contribute to each inclusive cross section at $\epsilon \sim 0$. The basic subprocesses expected in the CIM, and the resulting form of the inclusive cross section $Ed\sigma/d^3p \sim (p_\perp^2)^{-N}\epsilon^P$ for $p_\perp^2 \sim \infty$, $\epsilon \rightarrow 0$, and fixed $\theta_{c.m.}$ are given in the last columns. The subprocesses that have the dominant $p_\perp$ dependence at fixed ϵ are underlined. For some particular final-state quantum numbers, the above powers of ϵ should be increased.

Inclusive process	Exclusive-limit channel	Subprocesses	$\dfrac{d\sigma}{d^3p/E}$ $(\theta \sim 90°)$
$M + B \rightarrow M + X$	$M + B \rightarrow M + B*$ $(n = 10)$	$\underline{M + q \rightarrow M + q}$	$(p_\perp^2)^{-4}\epsilon^3$
		$\bar{q} + B \rightarrow M + qq$	$(p_\perp^2)^{-6}\epsilon^1$
		$M + B \rightarrow M + B*$	$(p_\perp^2)^{-8}\epsilon^{-1}$
$B + B \rightarrow B + X$	$B + B \rightarrow B + B*$ $(n = 12)$	$\underline{B + q \rightarrow B + q}$	$(p_\perp^2)^{-6}\epsilon^3$
		$\underline{(qq) + (qq) \rightarrow B + q}$	$(p_\perp^2)^{-6}\epsilon^3$
		$\underline{B + (qq) \rightarrow B + qq}$	$(p_\perp^2)^{-8}\epsilon^1$
		$\underline{B + B \rightarrow B + B*}$	$(p_\perp^2)^{-10}\epsilon^{-1}$
	$B + B \rightarrow B + B* + M*$ $(n = 14)$	$\underline{q + q \rightarrow B + \bar{q}}$	$(p_\perp^2)^{-4}\epsilon^7$
		$q + (qq) \rightarrow B + M*$	$(p_\perp^2)^{-6}\epsilon^5$
		$(qq) + B \rightarrow B + M* + qq$	$(p_\perp^2)^{-10}\epsilon^1$
		$B + B \rightarrow B + B* + M*$	$(p_\perp^2)^{-12}\epsilon^{-1}$
$B + B \rightarrow M + X$	$B + B \rightarrow M + B* + B*$ $(n = 14)$	$\underline{q + (qq) \rightarrow M + B*}$	$(p_\perp^2)^{-6}\epsilon^5$
		$q + B \rightarrow q(\rightarrow M + q) + B*$	$(p_\perp^2)^{-6}\epsilon^5$
		$q + B \rightarrow M + q + B*$	$(p_\perp^2)^{-8}\epsilon^3$
		$(qq) + B \rightarrow M + B* + qq$	$(p_\perp^2)^{-10}\epsilon^1$
		$B + B \rightarrow M + B* + B*$	$(p_\perp^2)^{-12}\epsilon^{-1}$
	$B + B \rightarrow M + M* + B* + B*$ $(n = 16)$	$\underline{M + q \rightarrow M + q}$	$(p_\perp^2)^{-4}\epsilon^9$
		$q + q \rightarrow \bar{q}(\rightarrow M + \bar{q}) + B*$	$(p_\perp^2)^{-4}\epsilon^9$
		$q + q \rightarrow M + B* + \bar{q}$	$(p_\perp^2)^{-6}\epsilon^7$
		$M + B \rightarrow M + B*$	$(p_\perp^2)^{-8}\epsilon^5$
	$B + B \rightarrow M + M* + M* + B* + B*$ $(n = 18)$	$\underline{q + \bar{q} \rightarrow M + M*}$	$(p_\perp^2)^{-4}\epsilon^{11}$
		$\underline{q + M \rightarrow q(\rightarrow M + q) + M*}$	$(p_\perp^2)^{-4}\epsilon^{11}$
$B + B \rightarrow \overline{B} + X$	$B + B \rightarrow \overline{B} + B* + B* + \overline{B}*$ $(n = 18)$	$\underline{q + q \rightarrow B* + \bar{q}(\rightarrow \overline{B} + qq)}$	$(p_\perp^2)^{-4}\epsilon^{11}$
		$q + q \rightarrow B* + \overline{B} + qq$	$(p_\perp^2)^{-8}\epsilon^7$
		$q + (qq) \rightarrow \overline{B} + B* + B*$	$(p_\perp^2)^{-10}\epsilon^5$

TABLE II. The expected dominant subprocesses for selected electromagnetically induced reactions at large transverse momentum. (See Table I.)

Inclusive process	Exclusive-limit channel	Subprocesses	$\dfrac{d\sigma}{d^3p/E}$ $(\theta \sim 90°)$
$\gamma + B \to \gamma + X$	$\gamma + B \to \gamma + B*$ $(n = 8)$	$\gamma + q \to \gamma + q$	$(p_\perp^2)^{-2} \epsilon^3$
		$\bar{q} + B \to \gamma + (qq)$	$(p_T^2)^{-5} \epsilon^0$
		$\gamma + B \to \gamma + B*$	$(p_\perp^2)^{-6} \epsilon^{-1}$
	$\gamma + B \to \gamma + B* + M*$ $(n = 10)$	$q + (qq) \to B* + \gamma$	$(p_\perp^2)^{-5} \epsilon^2$
		$q + B \to B* + \gamma + q$	$(p_\perp^2)^{-7} \epsilon^0$
		$\bar{q} + q \to M + \gamma$	$(p_\perp^2)^{-3} \epsilon^4$
		$\gamma + (qq) \to B* + \gamma + \bar{q}$	$(p_\perp^2)^{-6} \epsilon^1$
$\gamma + B \to M + X$	$\gamma + B \to M + B*$ $(n = 9)$	$\gamma + q \to M + q$	$(p_\perp^2)^{-3} \epsilon^3$
		$\bar{q} + B \to M + qq$	$(p_\perp^2)^{-6} \epsilon^0$
		$\gamma + B \to M + B*$	$(p_\perp^2)^{-7} \epsilon^{-1}$
	$\gamma + B \to M + M* + B*$ $(n = 11)$	$\gamma + (qq) \to B* + M + \bar{q}$	$(p_\perp^2)^{-7} \epsilon^1$
		$\bar{q} + q \to M + \bar{M}*$	$(p_\perp^2)^{-4} \epsilon^4$
		$q + (qq) \to M + B*$	$(p_\perp^2)^{-6} \epsilon^2$
$\gamma + B \to B + X$	$\gamma + B \to B + M*$ $(n = 9)$	$\gamma + (qq) \to B + \bar{q}$	$(p_\perp^2)^{-5} \epsilon^1$
		$q + B \to B + q$	$(p_\perp^2)^{-6} \epsilon^0$
		$\gamma + B \to B + M*$	$(p_\perp^2)^{-7} \epsilon^{-1}$
	$\gamma + B \to B + M* + M*$ $(n = 11)$	$q + q \to B + \bar{q}$	$(p_\perp^2)^{-4} \epsilon^4$
		$\gamma + q \to B + \bar{q}q$	$(p_\perp^2)^{-5} \epsilon^3$
		$q + (qq) \to B + M*$	$(p_\perp^2)^{-6} \epsilon^2$
$e + B \to e + X$	$e + B \to e + B*$ $(n = 8)$	$e + q \to e + q$	$(p_\perp^2)^{-2} \epsilon^3$
	$e + B \to e + B* + M* + M*$ $(n = 12)$	$e + \bar{q} \to e + \bar{q}$	$(p_\perp^2)^{-2} \epsilon^7$

e^+e^- annihilation. Finally, as illustrated in Fig. 4(c), we note that the hadron C can be emitted as a decay product from a hadron c of higher momentum. However, this should be less probable in high-momentum processes since the required subprocess must occur at a larger s_{ab}, and the cross sections have power-law falloff in s_{ab} at large angles. The $G_{a/A}(x)$ are also required at even larger values of x.

By using dimensional counting, the power-law behavior of the inclusive cross section can be related to the number of constituent fields involved in the basic large-transverse-momentum event. Representative lists of dominant subprocesses are given in Tables I and II, together with the associated power-law behavior. Several of the subprocesses have been discussed in detail in Refs. 9, 10, and 12.

These tables are constructed in the following manner. For each inclusive process $A + B \to C + X$ we first list the minimal exclusive channels $X = D$ (e.g., X is a baryon resonance or baryon $B*$ for $M + B \to M + X$). Using dimensional counting at the exclusive boundary ($\mathfrak{M}^2$ fixed, $p_T^2 \to \infty$) we have

$$\frac{d\sigma}{dt\,d\mathfrak{M}^2} \cong (p_T^2)^{2-n} f(t/s) ,$$

where n is the number of elementary fields in

A, B, C, and D. We next identify the leading CIM subprocesses (allowed by the exchange or interchange of quark fields using the elementary two-field meson and three-field baryon wave functions) which can connect to the exclusive-limit channel (e.g., $M + q \to M + q$ for $M + B \to M + B$). For each subprocess we have the contribution ($p_T^2 \to \infty$, $\epsilon = \mathfrak{M}^2/s$ fixed)

$$E \frac{d\sigma}{d^3p} = \frac{s}{\pi} \frac{d\sigma}{dt\,d\mathfrak{M}^2}$$

$$= \frac{1}{(p_T^2)^N} f\left(\frac{\mathfrak{M}^2}{s}, \frac{t}{s}\right)$$

$$\propto \frac{1}{(p_T^2)^N} \epsilon^P ,$$

where $N + 2$ is the number of fields in the subprocess $a + b \to c + d*$, and for $\theta_{c.m.}$ fixed ($\sim 90°$, for example)

$$P = g(a/A) + g(b/B) + g(c/C) + 1$$

$$= 2n_{\text{spect}} - 1 ,$$

where $n_{\text{spect}} = n(\bar{a}A) + n(\bar{b}B) + n(\bar{c}C)$ is the number of "spectator" fields. Note the identity[14]

$$N + P = n - 3 ,$$

which is the realization of the correspondence principle. The smooth connection between the

exclusive cross section (fixed $\mathfrak{M}^2$) and the $\epsilon \to 0$ limit of the corresponding inclusive cross section also can provide a rough normalization of each subprocess contribution to inclusive scattering. Note that the final-state hadrons in the exclusive-limit channel may recombine, but the resulting contribution is nonleading for this simpler process because it retains its overall scaling law $(p_T^2)^{2-n}$.

Table I describes hadronic processes and Table II gives typical electromagnetic processes. The entries that are underscored are the leading subprocesses for $p_T^2 \to \infty$, at fixed $\mathfrak{M}^2/s$. In the purely hadronic reactions, the leading subprocess have $N = 4$. Meson photoproduction has $N = 3$ and Compton scattering has a scale-invariant contribution with $N = 2$.

Generally, we expect that for ϵ not near 1 the dominant subprocesses are those that contribute to the exclusive-limit channels with the minimum value of n. For example, if this conjecture is true, the process $B + B \to B + X$ will have a small-$(p_T^2)^{-4}$ contribution which arises only from the subprocess $q + q \to B + \bar{q}$. Another particularly important example to check is the process $B + B \to M + X$. We emphasize that for $\epsilon \to 0$ (e.g., $x_T \to 1$ at 90°) a nonleading term in p_T^2 may become the most important because of a slower fall-off near $\epsilon \approx 0$. For $B + B \to M + X$, we have two main contributions at 90°

$$\sim \frac{h_1}{(p_T^2)^4} \epsilon^9 + \frac{h_2}{(p_T^2)^6} \epsilon^5 + O(p_T^{-16}) .$$

Higher powers of ϵ are predicted in certain cases; e.g., if $M = K^-$. The second contribution, which has a smaller sum $N + P$, becomes relatively more important as we move toward the exclusive limit. This could readily account for why the FNAL measurements[2] of $pp \to \pi^{\pm} X$ show a value $N \sim 5.5$ for $x_T > 0.4$, whereas the CERN ISR measurements at $x_T < 0.4$ for $pp \to \pi^0 X$ give the value $N \sim 4$. We discuss this further in Sec. IV. Notice that for the second contribution, a baryon system takes up the recoil momentum of the detected meson. For the dominant contribution which involves the subprocess $M + q \to M + q$, the recoil momentum is distributed in a "quark jet." Therefore it may be possible to separate these experimentally by examining the details of the final states and comparing with the final states in electroproduction.

Similarly, in inclusive meson photoproduction and inclusive Compton scattering, nonleading terms in p_T^{-2} may be important in the small-ϵ region (see Table II). The vector-dominance contributions are contained in the nonleading processes where the photon acts as a quark pair rather than a single elementary field. No specific references shall be made to these processes, but

all our formulas can be applied to them by using Table II as a guide.

C. Hadron and hadron-decay distributions in a general frame

Although the function $G_{a/A}(x)$ describes the fractional longitudinal momentum probability distribution in a frame in which $p_A \to \infty$, in fact, it is possible to determine some important features of G from measurements in a general frame, including the rest frame of A. This technique may be of considerable interest in the study of the decays of systems with a large Q value, such as the time-like photon in $e^+ e^-$ annihilation,[25] the (hadronic) system produced in $\bar{N}N$ annihilation,[26] and perhaps the decay of massive coherent states produced by diffractive excitation processes. The function $G_{a/A}(x)$ is introduced to describe the breakup of A into off-shell states which include a and the remainder $X(\bar{a}A)$. However, the decay of a very unstable system can reflect many of the properties of G, in particular, the threshold behavior.

In the general case, one can introduce the differential decay rate of particle A with mass A for the process $A \to a + X$, expressed in terms of the familiar c.m. variable $\omega = 2k_a^0/A$, as

$$\frac{d\Gamma}{d\omega} \equiv d_{a/A}(\omega) . \tag{16}$$

The decay is of course angularly symmetric in the rest frame of A. In order to bring about a closer analogy to the infinite-momentum-frame distributions, it is necessary to introduce an arbitrary (but fixed) z axis and to define $x = (k_a^0 + k_a^z)/A$. The decay distribution in this variable is

$$\frac{d\Gamma}{dx} \equiv D_{a/A}(x)$$

$$= \int_0^1 d\omega \left(\omega^2 - \frac{4a^2}{A^2} \right)^{-1/2} d_{a/A}(\omega) \, \theta \left(\omega - x - \frac{a^2}{A^2 x} \right).$$

The x distribution is peaked at $x = a/A$, and vanishes if x is too close to 0 or 1.

The function $d_{a/A}(\omega)$ is clearly the optimum distribution to measure experimentally, but, as we shall show in detail, $D_{a/A}(x)$ is in closer analogy to the infinite-momentum-frame distributions, such as $G_{a/A}(z)$, which are used in scattering processes.

Rather than discussing a very general model of such unstable systems, the physical point to be made here can be best illustrated by constructing a representative analytic function for the probability distribution using the form-factor diagram. The probability function is defined by (see Ref. 10 for details)

$$2p_A^\mu \int_0^1 dx\, G_{a/A}(x)$$

$$= i \int d^4k\, db^2\, \frac{2k^\mu \phi^2(k^2-a^2)\rho(b^2)}{[k^2-a^2]^2\,[(p_A-k)^2-b^2]} \quad , \quad (17)$$

where the spectrum of "core" masses b^2 is chosen to reflect the Regge behavior of the forward amplitude $\bar{a}A \to \bar{a}A$, i.e., $\rho(b^2) \sim (b^2)^\alpha$, and $\rho(b^2)$ vanishes for $b^2 < \mu^2$ but is finite at $b^2 = \mu^2$. The simplicity of this model arises from the assumption that the falloff of the vertex function ϕ does not depend on b^2.

We now introduce the general frame[8, 17]

$$p_A = (P + A^2/4P,\, \vec{0}_T,\, P - A^2/4P) \ ,$$

$$k = (xP + (k^2 + \vec{k}_T^2)/4xP,\, \vec{k}_T,\, xP - (k^2 + k_T^2)/4xP) \ ,$$

and   (18)

$$\int d^4k = \int d^2k_T \int_{-\infty}^\infty \frac{dx}{2|x|} \int_{-\infty}^\infty dk^2 \ ,$$

where A is the mass of particle A. This defines an arbitrary frame under the restriction that A is moving in the z direction, and $y = \ln(2P/A)$ is the rapidity of A. The rest frame of A is given by $P = \frac{1}{2}A$ and the infinite-momentum frame by $P \to \infty$. The k^2 integration can be carried out and one finds

$$G_{a/A}(x) = \frac{x}{2(1-x)} \int d^2k_T\, db^2 \rho(b^2)\, \phi^2(xS)\,[xS]^{-2} \ ,$$

where x must be between 0 and 1 and

$$S(\vec{k}_T, x) = A^2 - \frac{a^2 + \vec{k}_T^2}{x} - \frac{b^2 + \vec{k}_T^2}{1-x} \ .$$

This is the distribution function in x, where $x \equiv (k^0 + k^z)/(p_A^0 + p_A^z)$, in the arbitrary frame defined by the parameter P.

If the vertex function is taken to be $\phi(K^2) = (K^2)^{1-n}$, then the $\vec{k}_T$ integration can be carried out and one finds

$$G_{a/A}(x) \propto x^{2-2n} \int_{\mu^2}^\infty db^2\, \rho(b^2)\,[S(\vec{0}_T, x)]^{1-2n} \ .$$

The limiting behavior of G is then found to be

$$G \sim (1-x)^{2n-1}, \quad \text{for } x \sim 1$$

$$\sim x^{-\alpha}, \qquad\quad \text{for } x \sim 0$$

which is of the correct form and leads to the identification $n = n(\bar{a}A)$, as defined in Eq. (8).

The decay distribution function is most easily computed by evaluating the absorptive part of the self-energy diagram. The total decay width is proportional to

$$\Gamma \propto \text{Im}\, i \int d^4k\, db^2\, \frac{\rho(b^2)\,\phi^2(k^2-a^2)}{[k^2-a^2]\,[(p_A-k)^2-b^2]} \ ,$$

which, proceeding as before, becomes $[S = S(\vec{k}_T, y)]$

$$\Gamma \propto \text{Im} \int \frac{dy}{1-y}\, d^2k_T\, db^2\, \rho(b^2)\, \phi^2(yS)\,[yS]^{-1} \ .$$

If ϕ is chosen as before, then the k_T^2 integration can be performed and taking the imaginary part $(A^2 \to A^2 - i\epsilon)$ yields

$$\Gamma \propto \int_0^1 dy\, y^{2-2n} \int_{\mu^2}^\infty db^2\, \rho(b^2)\,(-)^{2n-3}$$

$$\times \delta^{(2n-3)}\,(S(\vec{0}_T, y)) \ ,$$

where the $(2n-3)$ derivative of the δ function must be evaluated. The argument of the δ function allows the identification of y as the familiar (center-of-mass) variable ω, i.e., $y = \omega \equiv 2E_a/A$. Then the differential rate is

$$\frac{d\Gamma}{d\omega} \propto \left(\frac{1-\omega}{\omega}\right)^{2n-2} \rho^{(2n-3)}\,[b^2(\omega)] \ , \qquad (19)$$

where $b^2(\omega) \equiv (1-\omega)(A^2 - a^2/\omega) \geq \mu^2$ and the $(2n-3)$ derivative of $\rho(b^2)$ is needed. This threshold behavior is not the same as $G_{a/A}(x)$ because the ω variable is essentially a radial variable in the spatial momentum of particle a. It may be interesting to fit data with the model form of Eq. (19) which predicts relations between conjugate values of ω, i.e., those values of ω which produce the same value of $b^2(\omega)$.

One should also note that if the distribution $\rho(b^2)$ has a δ-function contribution (corresponding to a two-particle decay mode) the corresponding value of ω is fixed kinematically so the above distribution function is not interesting. We are assuming, in effect, that there is an extended type of "duality," in which there is an effectively smooth mass distribution function $\rho(b^2)$ which describes the decay at any fixed ω value. This assumption clearly improves as the ratio (A/μ) increases, which allows many particle decay modes to occur and to dominate.

The corresponding infinite-momentum-like distribution is achieved by defining a z axis arbitrarily and projecting all events onto this axis. Introducing the variable x as before, the differential rate is (neglecting final masses for the moment)

$$\frac{d\Gamma}{dx} \equiv D_{a/A}(x) \approx \int_x^1 \frac{d\omega}{\omega}\, d_{a/A}(\omega)$$

and one finds that as $x \to 1$,

$$D_{a/A}(x) \sim (1-x)^{2n-1} \ . \qquad (20)$$

This is the same threshold behavior as we found for $G_{a/A}(x)$. The Regge behavior of $\rho(b^2)$ may not play a role here because the maximum value of $b^2(\omega)$ that can be reached occurs for $\omega = a/A$, and $b_{\max}^2 \sim (A-a)^2$. This may or may not be in the Regge region, depending on the dynamics involved.

One sees that a measurement of the decay functions $d_{a/A}(\omega)$ and $D_{a/A}(x)$ can provide important information on and confirmation of the dynamical assumptions used in the CIM. For example, the prediction for the process $N\bar{N} \to \pi X$ in $n(\pi N\bar{N}) = 2$, and hence $D_{\pi/N\bar{N}}(x) \sim (1-x)^3$. The prediction of the process $e^+e^- \to "\gamma" \to \pi X$ is $n(\pi\gamma) = \frac{3}{2}$ if the photon is regarded as an elementary field, and $n(\pi\gamma) = 2$ if the photon is completely described by vector-meson dominance. The ω distribution $d_{\pi/\gamma}(\omega)$ is predicted to vanish as $(1-\omega)^1$, which is the expected behavior in a parton model for $\nu\bar{W}_2(\omega)$. We note, however, that the threshold behavior can be modified by spin effects. Various model calculations for νW_2^π have been reviewed by Ezawa.[14]

III. THE EXCLUSIVE-INCLUSIVE CONNECTION

In this section we shall investigate the connecting links between the exclusive cross section and low-missing-mass inclusive processes. Further, we will derive correction terms to the usual triple-Regge formula which are required in order that the triple-Regge cross section will have the correct exclusive limit at any momentum transfer.

Let us consider the inclusive process $A + B \to C + X$ near the exclusive limit ($\epsilon = \mathfrak{M}^2/s \ll 1$), of the Peyrou plot, and we will choose $x_L > 0$. Thus we can ignore hadronic bremsstrahlung from A; only the contribution $G_{a/A} \propto \delta_{aA}\delta(1-x)$ needs to be considered.

Let us first consider the case of large transverse momentum with $\epsilon \ll 1$, $x_L > 0$. Of the subprocesses shown in Fig. 3, the simple interchange subprocess of Fig. 3(a) based on $A + q \to C + q$ is generally most important. Using Eq. (4) we have for

$$R \equiv s\frac{d\sigma}{d^3p/E} = \frac{s^2}{\pi}\frac{d\sigma}{dt\,d\mathfrak{M}^2} \tag{21}$$

the contribution

$$\frac{1}{\pi}\frac{s^2}{s+u} x\, G_{q/B}(x) \frac{d\sigma}{dt}(A+q \to C+q)\Big|_{\substack{s'=xs \\ t'=t}} . \tag{22}$$

(A summation over contributing quark types is assumed.) The function $G_{q/B}$ *includes* the reducible contribution from the fragmentation of the target B.

As we have noted, the quark-hadron cross section in the CIM takes a simple Regge form ($s' \to \infty$, $t \to \infty$)

$$\frac{d\sigma}{dt}(q+A \to q+C)$$

$$\simeq |\gamma(t)(-u')^{\alpha_{AC}(t)} + \bar{\gamma}(t)(-s')^{\alpha_{AC}(t)}|^2/s'^2, \tag{23}$$

where for large $-t$, the trajectory function α_{AC} approaches the negative integer $\alpha_{AC}(-\infty) = 1 - \frac{1}{2}(n_A$

$+n_C)$ and $\gamma(t)$, $\bar{\gamma}(t)$ become asymptotically constant. For example, for quark-meson scattering, we have the limiting behavior $\alpha^{I=0}(-\infty) = \alpha^{I=1}(-\infty) = -1$. (Alternatively, as developed in Ref. 8, we can obtain the asymptotic trajectories of the $q+A \to q+C$ amplitude from the power-law behavior of the form factors of A and C, assuming a quark-core bound-state model for the hadrons.) As the momentum transfer becomes smaller, the contributions from virtual hadronic bremsstrahlung [as shown in Fig. 3(c)] Reggeize the amplitude and move the trajectories and residue functions away from their asymptotic value. This effect has been computed and examined in detail in Ref. 17. The detailed manner in which the $\alpha(t)$ and $\gamma(t)$ approach their limiting values, although not needed for our discussion here, can be computed. The effects due to the coupled-channel effect of the Reggeization process is sometimes important, especially for the cases in which A and C are both baryons. In general, we can treat $\alpha_{AC}(t)$ as an effective trajectory, constrained to fit its experimental value at $t = 0$ as required by the analyses of exclusive processes, and its asymptotic value at $t \to -\infty$ determined from constituent structure.

For the form of the quark structure function, we use the simplified structure

$$xG_{q/B}(x) \sim F_{2B}(x) = x^{1-\alpha_B(0)}(1-x)^{2B-1}, \tag{24}$$

with $\alpha_B(0) \sim 1$ representing the Pomeron behavior, and the threshold behavior given by the Drell-Yan relation for the form factor

$$F_B(t) \sim (-t)^{-B} .$$

Dimensional counting gives the value of B: $1+B$ = number of quark fields in the simplest configuration in the state B.

The inclusive cross section then becomes

$$R_r = \frac{s^2}{\pi(s+u)}\left(\frac{\mathfrak{M}^2}{\mathfrak{M}^2-t}\right)^{2B-1} x^{1-\alpha_B(0)}\frac{\gamma^2(t)}{(xs)^2}(-xu)^{2\alpha_{AC}(t)}$$

$$= s^{\alpha_B(0)}\left(\frac{-u}{s}\right)^{1+\alpha_B(0)}\frac{\gamma^2(t)}{\pi p_T^2}\left(\frac{\mathfrak{M}^2}{\mathfrak{M}^2-t}\right)^{2B-1}$$

$$\times\left(\frac{\mathfrak{M}^2-t}{sp_T^2}\right)^{\alpha_B(0)-2\alpha_{AC}(t)}, \tag{25}$$

where for simplicity we only display the $\gamma(t)(-u')^{\alpha_{AC}(t)}$ contribution. Note that R_r gives the Reggeized inclusion cross section including the reducible contributions from the target B, but contains only the virtual hadronic bremsstrahlung contributions for A. This is, of course, the same as the single-diffractive scattering terms in ordinary Mueller-Regge analysis.

In the triple-Regge region, defined by the conditions $s \sim |u| \gg \mathfrak{M}^2 > |t|$, Eq. (25) achieves the

familiar form

$$R_r \sim s^{\alpha_B(0)} \left(\frac{\mathfrak{M}^2 - t}{s}\right)^{\alpha_B(0) - 2\alpha_{AC}(t)} \beta(t) \,,$$

where $\qquad\qquad\qquad\qquad\qquad$ (26)

$$\beta(t) \cong \frac{\gamma^2(t)}{\pi} (-t)^{2\alpha_{AC}(t) - \alpha_B(0) - 1} \,.$$

Note that in the triple-Regge limit, the threshold behavior of $F_{2B}(x)$ is irrelevant since

$$x = - t/(\mathfrak{M}^2 - t) \to 0.$$

In contrast, the exclusive limit of R_r is attained by integrating over a finite range of small values of the missing mass $\mathfrak{M}$. In this region, the threshold behavior of $F_{2B}(x)$ is crucial, and one finds

$$\frac{d\sigma}{dt} = \pi \int d\mathfrak{M}^2 \frac{R_r}{s^2}$$

$$\sim \frac{\gamma^2(t)}{s^2} F_B{}^2(t)(-u)^{2\alpha_{AC}(t)} \,. \qquad (27)$$

This gives the correct exclusive Regge form and the correct large-angle limit for the exclusive cross section. The complete signatured Regge trajectories are restored when we include the $\tilde{\gamma}(t)(-s')^{\alpha_{AC}(t)}$ terms in Eq. (23).

This smooth joining of inclusive to exclusive scattering is the strong interaction analog of Bloom-Gilman duality as was discussed in Refs. 8 and 16. This kinematic region requires values of x near 1 and hence depends sensitively on the threshold behavior of $F_{2B}(x)$. Since the triple-Regge limit does not retain this behavior, it will *not* join smoothly onto exclusive scattering. To clarify this point, note that if we expand the structure function of the target,

$$\left(\frac{\mathfrak{M}^2}{\mathfrak{M}^2 - t}\right)^{2B-1} = \left(1 + \frac{t}{\mathfrak{M}^2 - t}\right)^{2B-1}$$

$$= 1 + (2B - 1)\frac{t}{\mathfrak{M}^2 - t} + \cdots \,,$$

then we see that this correction factor gives rise to contributions to the triple-Regge formula at $\alpha_B(0)$, $\alpha_B(0) - 1$, $\alpha_B(0) - 2, \ldots$, with residues in the ratio 1, $(2B - 1)t, \ldots$. The proper threshold behavior is then seen to require the cooperative effort of at least $2B$ trajectories. These correction terms are important in the small-$\mathfrak{M}^2$, large-t sector of the triple-Regge region. This is another

example of how a power-law falloff of amplitudes in the deep-scattering region forces relations between the residues and trajectories of the leading and nonleading Regge contributions.

Note that for fixed $\mathfrak{M}^2$ and t, with $s \to \infty$, the threshold dependence of R_r,

$$R_r \sim \left(\frac{\mathfrak{M}^2}{s}\right)^{n(t)} = \epsilon^{n(t)}, \quad \epsilon \to 0 \qquad (28)$$

is related to the leading Regge behavior in the $\overline{A}C$ channel:

$$n(t) = \alpha_B(0) - 2\alpha_{AC}(t)$$

$$\cong 1 - 2\alpha_{AC}(t) \,.$$

This is in agreement with the $t = 0$ result obtained by Feynman,[27] Mueller,[19] and Bjorken and Kogut.[16]

IV. THE INCLUSIVE CROSS SECTION IN THE INTERIOR REGION

Except for the limited region where $\epsilon \to 0$, that is throughout the entire central region of the Peyrou plot, the effects of hadronic bremsstrahlung from both the projectile A and target B must be taken into account. We can write the full cross section in the form

$$R_c(A + B \to C + X)$$

$$= \sum_H \int_{z_0}^1 \frac{dz}{z} G_{H/A}(z) R_r(H + B \to C + X') \Big|_{\substack{s'=zs \\ u'=u;\ t'=zt}} , \qquad (29)$$

where $z_0 = -u/(x+t)$, and R_r is the cross section discussed in Sec. III for the scattering of the hadron-irreducible states H. The subscript c indicates the central-region cross section. Note that the symmetry between the particles A and B is not explicit in Eq. (29). However, in the forward direction, this is convenient form since it allows an expansion in the natural Regge trajectories in $R_r(H + B \to C + X')$. In the backward direction, one must interchange the roles of A and B. Both expressions must be used and will smoothly merge in the region near 90°.

Using Eq. (25), which is based on the underlying subprocesses of Figs. 3(a) and 3(c), we have for $x_L > 0$ and $p_T{}^2$ large

$$R_c(A + B \to C + X) = \sum_H \frac{s^{\alpha_B(0)}}{p_T{}^2} x_1{}^{1 + \alpha_B(0)} (1 - x_2)^{2B-1} \int_{z_0}^1 \frac{dz}{z^2} G_{H/A}(z) \left(\frac{z - z_0}{z - x_1}\right)^{2B-1} \left(\frac{z - x_1}{z p_T{}^2}\right)^{\alpha_B(0) - 2\alpha_{HC}(zt)} \gamma^2(zt) \,,$$

$$(30)$$

where the dimensionless variables are defined by

$$x_1 = -u/s, \quad x_2 = -t/s ,$$

$$z_0 = \frac{x_1}{(1 - x_2)}, \quad \epsilon = \mathfrak{M}^2/s = 1 - x_1 - x_2 .$$

As usual, the particle masses have been ignored. The longitudinal fraction x_L (Feynman x) and x_T are given by

$$x_L = x_1 - x_2, \quad x_T^2 = 4x_1 x_2,$$

$$\epsilon = 1 - (x_T^2 + x_L^2)^{1/2} , \tag{31}$$

and the inverse relations are

$$2x_1 = (x_T^2 + x_L^2)^{1/2} + x_L ,$$

$$2x_2 = (x_T^2 + x_L^2)^{1/2} - x_L .$$

Let us now examine R_c in several kinematic limits in order to compare the behavior of the various contributions. In the central Regge or pionization region defined by

$$x_1, x_2 \sim O\left(\frac{1}{\sqrt{s}}\right) ,$$

i.e.,

$$\epsilon \sim 1, \quad p_T^2 \sim \text{constant},$$

we obtain for large p_T^2

$$R_c = \sum_H \frac{s^{[\alpha_A(0) + \alpha_B(0)]/2}}{(p_T^2)^{1 + [\alpha_A(0) + \alpha_B(0)]/2 - 2\bar\alpha_{HC}}} \Gamma_H(x_L, \theta_{c.m.}) , \tag{32}$$

where $\theta_{c.m.} = \tan^{-1}(x_T/x_L)$ is the center-of-mass scattering angle and the trajectory $\bar\alpha_{HC} = \alpha_{HC}(\bar z t)$ has been evaluated at some average point $\bar z$ of the integral $(\bar z |t| > x_L |t| \cong p_T^2)$. The fragmentations of both A and B contribute equally to the Regge behavior of $R_c \sim s^{[\alpha_A(0) + \alpha_B(0)]/2} \sim s^1$, as expected.

The leading contributions to R_c for the process $p + p \to \pi + X$ will be the quark-meson scattering subprocesses (see Table I) with

$$\bar\alpha_{HC}(-\infty) = \alpha_{M\pi}(-\infty) = -1 .$$

The inclusive cross section also includes background terms arising from the subprocesses

$$q + (q\bar q) \to M + B^*$$

and

$$q + B \to q + B^*$$
$$\searrow M + q .$$

The total result is of the form

$$E \frac{d\sigma}{d^3p} = \frac{1}{p_T^8} H^M(x_T, \theta_{c.m.}) + \frac{1}{p_T^{12}} H^B(x_T, \theta_{c.m.}) , \tag{33}$$

which for $\theta_{c.m.} \sim \frac{1}{2}\pi$ and $x_T \sim 1$ has the behavior

$$E \frac{d\sigma}{d^3p} \sim \frac{1}{p_T^8}(1 - x_T)^9 h^M + \frac{1}{p_T^{12}}(1 - x_T)^5 h^B .$$

Detailed calculations[17] for these subprocesses have been carried out using the *predicted* form of $G_{\pi/p}(z) \propto z^{-1}(1 - z)^5$ and $F_{2p}(x) \propto (1 - x)^3$. These results for $\theta_{c.m.} \sim 90°$ are in excellent agreement with the recent CERN ISR data[1] and in reasonable agreement with the FNAL data.[2] The only important undetermined parameters in this prediction are the overall normalizations. There is an additional mass parameter $M^2 \sim 0.71 \text{ GeV}^2$ which occurs in the assumed meson form factors, but the predictions for $p_T > 1 \text{ GeV}/c$ are independent of its value. At angles other than 90°, we must include the other topologically different contributions, including the full angular dependence of the quark-meson amplitude. That is, both the (ut) and (st) diagrams must be included in the R_r amplitude. Reasonable agreement can be achieved with the above form from 25 GeV/c, $0 < x_L \lesssim 0.5$, up to the CERN ISR data at $x_L = 0$.

It is strongly suggested by the lower-energy inclusive data[2,3] that there are important contributions for large x_T which fall as p_T^{-12}, as does the second term in Eq. (33). As we have emphasized in Sec. II B, these terms may be contributing to a substantial fraction of the measured rate at the large x_T's of the FNAL data. More extensive data at lower energies would be useful in separating these two types of important subprocesses.

By exposing the internal quark lines and the underlying quark-meson scattering subprocesses, one obtains the minimum falloff in p_T at fixed ϵ. Conversely, for fixed p_T, with $\epsilon \to 0$, graphs with the least possible fragmentation are favored. Thus the direct large-transverse-momentum processes involving the incident hadrons can be important, but at the expense of a larger falloff in p_T. The large-x_T (or small-ϵ) limit can therefore be quite different from the large-p_T limit. Let us thus examine the behavior of R_c in the threshold limit in order to establish counting rules which will allow us to enumerate the leading contributions in the various kinematic regions.

The leading threshold ($\epsilon \to 0$) behavior of R_c will depend critically on whether x_2 is large or small, as was the case for R_r. By changing the integration variables to $z = z_0 + y(1 - z_0)$, where $z_0 = x_1/(1 - x_2)$, R_c becomes

$$R_c = \sum_H s^{\alpha_B(0)} \frac{x_1^{1 + \alpha_B(0)}}{p_T^2 + M^2} (1 - z_0)^{g + 2B}(1 - x_2)^{2B - 1}$$

$$\times \int_0^1 dy \frac{(1 - y)^g y^{2B - 1}[x_2 z_0 + y(1 - z_0)]^{\alpha_B(0) + 1 - 2\alpha - 2B}}{[1 - (1 - z_0)(1 - y)]^{2(1 - \alpha) + \alpha_A(0) + \alpha_B(0)}[p_T^2 + M^2]^{\alpha_B - 2\alpha}} , \tag{34}$$

with $G_{H/A} \sim (1 - z)^g/z$, and $\alpha = \alpha_{HC}(zt)$. Using the mean-value theorem, R_c can be readily estimated; the controlling factors are $[\alpha_B(0) = 1]$

$$R_c = s \sum_H (M^2 + p_T^2)^{2(\bar{\alpha}-1)} \epsilon^{2B+g} (1 - x_1)^{2(1-\bar{\alpha}-B)} (1 - x_2)^{1-g} \left(\frac{x_1 x_2 + \bar{y}\epsilon}{x_1 x_2 + \epsilon}\right)^{2(1-\bar{\alpha}-B)} \left(\frac{x_1 + \epsilon}{x_1 + \bar{y}\epsilon}\right)^{2(1-\bar{\alpha})} , \tag{35}$$

where $\bar{\alpha} = \alpha(\bar{z}t)$, M is a mass characterizing the form factor of particles H and C, and we can estimate $\bar{y} = 2B/(2B + g + 1)$, $\bar{z} = (x_1 + \bar{y}\epsilon)/(1 - x_2)$. More generally, the contribution of any irreducible subprocess $a + b \rightarrow C + d^*$ for $x_L > 0$ is given by

$$\sim s \, \epsilon^{g(a/A)+g(b/B)+1} \left(\tfrac{1}{4} x_T^2 + \bar{y}\epsilon\right)^{1-g(b/B)-2\bar{\alpha}}$$

$$\times f(p_T^2, \theta_{c.m.}) , \tag{36}$$

where the large-p_T power dependence of f can be obtained via dimensional counting. If x_2 is large, which is the case in the transition and deep scattering regions, then as $\epsilon \rightarrow 0$, $\tfrac{1}{4} x_T^2 \gg \bar{y}\epsilon$, and

$$R_c \propto s \, \epsilon^{g(a/A)+g(b/B)+1} f(p_T^2, \theta_{c.m.}) .$$

Both a and b carry a large fraction of the incident hadron momenta in this kinematic region. On the other hand, for $x_T^2 \ll 4\bar{y}\epsilon$, which is required in order to approach the usual triple-Regge region, only particle a needs to carry a large longitudinal momentum and

$$R_c \propto s \, \epsilon^{[g(a/A)+2-2\bar{\alpha}_{aC}]} f(p_T^2) . \tag{37}$$

This can be interpreted as a triple-Regge formula with an effecitve trajectory

$$\alpha_{\text{eff}}(t) = \alpha_{aC}(\bar{z}t) - \tfrac{1}{2}[1 + g(a/A)] , \tag{38}$$

where $\bar{z} \cong x_L + \bar{y}(1 - x_L)$. Notice however, that α_{eff} corresponds to a disconnected cut contribution to the inclusive cross section (see Fig. 6) and has no analogue trajectory in an exclusive reaction. Note also that in the small-missing-mass region, these hadron-reducible contributions of R_c give rise to nonleading contributions to the exclusive cross section at fixed $\theta_{c.m.}$.

We have now identified two potentially important contributions to the triple-Regge formula; one is important at low missing mass (and provides the correct extrapolation to the exclusive limit), and the other, the double-bremsstrahlung contribution R_c is important at large missing mass (and provides the correct extrapolation into the central Regge or pionization region). The situation is schematically represented in Fig. 1, where the various regions are labeled by the dominant contribution. Some applications will be discussed in Sec. V.

Note also that Eq. (35) predicts that the powers of p_T^2 are not fixed but should vary with $\alpha(\bar{z}t)$ (which approaches a negative constant only at sufficiently negative values of its argument). For

example, if the region near the lower limit on the z integral dominates in Eq. (30), then $\bar{\alpha} \approx \alpha(-p_T^2/(1 - x_2))$, and this may be considerably larger than its asymptotic value. Thus the data are expected to show a variation in effective power of p_T^2 not only from the above effect at small p_T^2, but also from the sum over H which will contribute differing powers of p_T^2 and ϵ.

Finally, we note that the hadronic bremsstrahlung model and the predicted form for $G(z)$ allow one to understand in detail the almost kinematical origin of the approach to Feynman scaling. For example at $x_L = 0$, Eq. (37) for R_c can be expanded at fixed p_T in inverse powers of $\sqrt{s}$, and one finds

$$R_c \sim \sum_H s \, p_T^{4(\bar{\alpha}-1)} \left[1 - (g + 2 - 2\bar{\alpha}) \frac{2p_T}{\sqrt{s}} + \cdots\right] \Gamma^H .$$

The first term scales in the Feynman sense. The second term can be interpreted as a nonleading Regge contribution and one sees that it has a very large residue. For example, in the reaction $pp \rightarrow \pi X$, $g + 2 - 2\bar{\alpha} = 9$. The leading trajectories in exclusive and inclusive scattering must be equal;
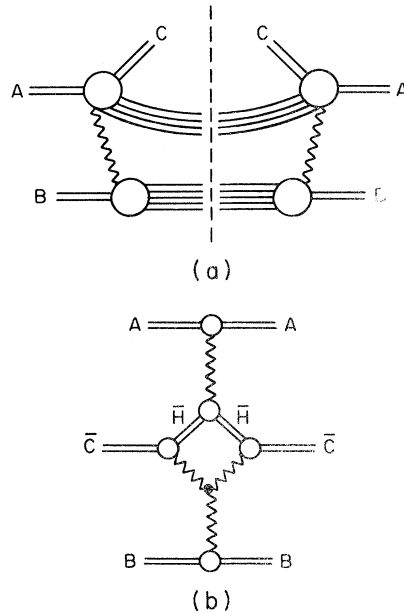
(a)

(b)

FIG. 6. The disconnected cut contributions to the inclusive cross section which arise from hadronic bremsstrahlung from both projectile and target. The nature of the final state is shown in Fig. 6(a). Alternatively, the inclusive cross section can be expressed as a Mueller discontinuity of the amplitude illustrated in Fig. 6(b).

the importance of secondaries can be quite different, however, and the resultant approach to the expected leading Regge behavior can be vastly different in the two cases. The above type of kinematic corrections, that control the approach to ultimate Regge power behavior, should occur in elastic scattering as well as inelastic, and may well be important there also.

V. APPLICATIONS TO LOW-MOMENTUM INCLUSIVE REACTIONS

As we have noted, the R_c term, which allows for hadronic bremsstrahlung from the projectile A, plays an important role throughout the entire central region, both in the pionization region of fixed momentum transfer $[x_L, x_T \sim O(1/\sqrt{s})]$, and in the large-transverse-momentum domain $[p_T \sim O(\sqrt{s}), \epsilon = \mathfrak{M}^2/s$ fixed$]$. Since the normal triple-Regge formulas ignore projectile fragmentation, it is a natural question whether the reducible processes play a significant role in the triple-Regge limit $(x_L \to 0, \epsilon \sim 1 - x_L$ fixed$)$ for inelastic processes. As we have shown in Sec. IV, the R_c cross section corresponding to Fig. 7(a), which is based on the irreducible subprocess $H + B \to C + X'$, has the threshold behavior $\epsilon^{g(H/A)+2(1-\alpha_{\bar{H}C})}$. For the diffractive case with $H = C$, we have at $t \to 0$, $R_{(a)} \sim \epsilon^{g(H/A)}$. The threshold dependence of the inclusive cross section thus directly depends on the threshold behavior of $G_{H/A}(z)$.[28]

In addition, at small t we must also consider the processes illustrated in Fig. 7(b) and 7(c). In Fig. 7(b), the projectile A diffractively scatters into a state $H = A$, which then decays into particle C. In this "diffractive excitation" process the probability of diffractive scattering with fractional momentum z is $(1-z)^{\alpha_B - 2\alpha_{AA}(t)}$, and the probability of decay to C is $G_{C/A}(x_L/z)$. Hence the overall behavior is given by the convolution

$$R_{(b)} \sim \int_{x_L}^{1} dz\,(1-z)^{\alpha_B - 2\alpha_{AA}(t)}$$
$$\times \left(1 - \frac{x_L}{z}\right)^{g(C/A)} \left(\frac{x_L}{z}\right)^{-\alpha_A}$$
$$\sim (1 - x_L)^N \quad (x_L \to 1), \tag{39}$$

where

$$N = \alpha_B + 1 - 2\alpha_{AA}(t) + g(C/A),$$

which has the same threshold dependence as $R_{(a)}$. In Fig. 7(c), the initial projectile emits C along the beam direction and the remaining fragments of A diffractively scatter from the target B. Again this gives the same result

$$R_{(c)} \sim (1 - x_L)^{g(C/A)}$$

in the threshold region and at $t \to 0$.
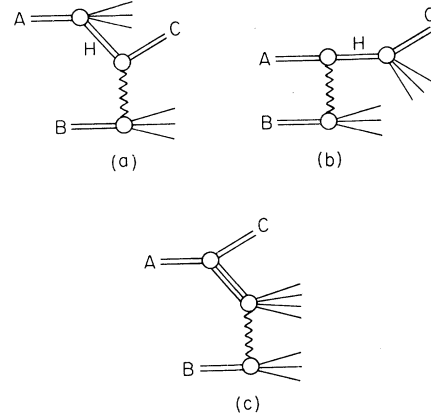

FIG. 7. The three major fragmentation contributions to the inclusive cross section $A + B \to C + X$ for $x_L \sim 1$ which are discussed in Sec. V.

Equation (38) for the threshold dependence of diagram 7(a), can be interpreted as yielding an effective trajectory

$$\alpha_{\text{eff}} = \alpha_{HC} - \tfrac{1}{2}[1 + g(H/A)] \tag{40}$$

in place of α_{AC} in the triplet-Regge formula. Although the dominant contribution at $t \to 0$ usually arises from the term with $H = C$, so that $\alpha_{CC}(0) = 1$ (Pomeron), one may have to pay the penalty of a large value for $g(C/A)$. For example, in the reaction $pp \to K^- X$, the choice $H = K^- = C$ yields a more rapidly vanishing contribution (lower α_{eff}) than does the choice $H = \pi$, using the leading strangeness changing $\alpha_{\pi k-}$ (presumably K^*) trajectory, since $g(K^-/p)$ is four units larger than $g(\pi/p)$. Notice, however, that the particle which balances strangeness is expected to show up in different hemispheres for these two terms, so in principle they can be separated experimentally.

Let us now look at the experimental situation. We shall use the phenomological analysis of the data[3] from inelastic pp reactions at 19.2 GeV/c and 30 GeV/c which was carried out by Chen, Wang, and Wong.[29] The comparison with the experimental values for the effective trajectory at $t = 0$ is shown in Table III. It should be stressed that in these data the ratio $\mathfrak{M}^2/s$ was not small, and hence one should expect corrections to the type that we have been discussing. The values given for α_{pC} are the usual predictions of the triple-Regge formula R_r assuming the conventional trajectories of exclusive processes. The predictions for α_{eff} are based on the diffractive contribution to R_c,

$$\alpha_{\text{eff}} = \tfrac{1}{2}[1 - g(C/A)]$$
$$= 1 - n(\bar{C}A),$$

as determined by dimensional counting (see Sec. II). Nonleading Regge terms, such as the ρ under the Pomeron, will also contribute, as always. The value $\alpha_{\text{eff}} \sim -3$ in the table for $pp \to K^- p$ is the prediction assuming $\alpha_{\pi K^-} \approx 0$.

Thus we find that the effective trajectory extracted from the data lies between the expected triple-Regge value α_{pC} and α_{eff}, and the predictions for the exotic channels are in good agreement with the predictions of the CIM. We therefore infer that the nonleading terms discussed above are of the same order of magnitude as the expected triple-Regge terms in this kinematic region. Clearly, a more extensive analysis over a larger energy and $\mathfrak{M}^2$ range is needed before any definite conclusion can be drawn.

Finally, it should be remarked that the correction to the triple-Regge term in the small-missing-mass region [see Eq. (25) and the following discussion] introduces a dependence on momentum transfer. This can affect the effective trajectory that describes the missing-mass dependence and may be quite important. This should be taken into account in analyses of inclusive data at only one energy (or a narrow range of energies) even for quite small values of t/M^2.

VI. DISCUSSION AND CONCLUSIONS

In this paper an attempt was made to unify the description and treatment of single particle inclusive scattering throughout the entire Peyrou plot. Important (nonleading) corrections to the

TABLE III. Regge behavior for the inclusive process $p + p \to C + X$. Column II gives the expected dominant Regge exchange at $t = 0$. The predictions of the CIM for the exotic trajectories α_{pK^-} and $\alpha_{p\bar{p}}$ are given in parenthesis. The quantity α_{eff}, as computed using Eq. (40), describes the behavior of R_c. The final column gives the experimentally observed effective trajectory as analyzed in Ref. 29.

C	α_{pC}	α_{eff}	$\alpha_{\exp}$ (Ref. 29)
p	$\alpha_{\text{Pom}} = 1, \frac{1}{2}, 0$	-1	-0.1
π^+	$\alpha_N = -0.4$	-2	-1.3
π^-	$\alpha_\Delta = +0.2$	-2	-2.0
K^+	? (~ -1)	-2	-1.1
K^-	exotic (> -3)	$\sim -3, -4$	-3.6
$\bar{p}$	exotic (> -4)	-5	-5.7

leading Mueller-Regge analysis were identified and described. These terms serve to join smoothly the various regions of the Peyrou plot. Two important results are (a) the correction at large missing mass in the triple-Regge region arising from the terms that dominate the central region and vice versa, and (b) the corrections at small missing mass in the triple-Regge region that allow the amplitude to join smoothly onto the exclusive scattering. This connection is valid at fixed angle or at fixed momentum transfer.

The above remarks are perhaps most easily summarized by our formula for the inclusive cross section $(A + B \to C + X)$, which in the triple-Regge region has the typical form

$$E\frac{d\sigma}{d^3p} = \left(\frac{\mathfrak{M}^2 - t}{s}\right)^{1-2\alpha(t)} \left(\frac{\mathfrak{M}^2}{\mathfrak{M}^2 - t}\right)^{g(a/B)} \left[\beta(p_T^2) + \sum_a H^a(p_T^2)\left(\frac{\mathfrak{M}^2 - t}{s}\right)^{2(\alpha - \bar{\alpha})}\left(\frac{\mathfrak{M}^2}{s}\right)^{1+g(a/A)} + (A \to B)\right],\qquad(41)$$

where $\alpha = \alpha_{AC}(t)$, $\bar{\alpha} = \alpha_{aC}(\bar{z}t)$, and for large p_T^2

$$H^a(p_T^2) \simeq (M^2 + p_T^2)^{2(\bar{\alpha} - 1)},$$

$$\beta(p_T^2) \simeq (M^2 + p_T^2)^{2(\alpha - 1)}.$$

Cross terms between different Regge trajectories and signatures have been ignored and only PPP and RRP terms are retained. The trajectories and residues must satisfy the limits described in Sec. II. There is some evidence from an analysis of inclusive data[30] that there are important contributions that increase rapidly as $\mathfrak{M}^2/s$ ($= 1 - x_L$) increases ($x \lesssim 0.7$, say). These do not seem to be easily accounted for from the standard PPR, PPR, RRP, RRR, $\pi\pi P$, and $\pi\pi R$ terms. It would be interesting to see if the additional contributions are consistent with (41) and extrapolate to small x_L and to large p_T with the proper normalization required by the data in these regions. It should

be noted that for very small t and $1 - x_L$, our approach is not incompatible with conventional duality arguments for inclusive processes. Duality for exclusive processes is discussed in Ref. 17.

To amplify our general result, the inclusive cross sections, at large angles in the center-of-mass frame, for the processes $pp \to Cx$, where $C = \pi, p, \bar{p}, K, \rho, \ldots$, are expected to be of the form

$$E\frac{d\sigma}{d^3p} = (m^2 + p_T^2)^{-4}H_1(x_T, \theta)$$

$$+ (m^2 + p_T^2)^{-6}H_2(x_T, \theta)$$

$$+ (m^2 + p_T^2)^{-8}H_3(x_T, \theta) + \cdots$$

where the variable dependences of the H's are predicted by the theory and can be read off from formulas given in the text for large x_T. H_2 is expected in general to vanish less rapidly than H_1

as $\epsilon \to 0$. At fixed x_T, the second term will vary as $\sim s^{-6}$ while the first term varies approximately as $\sim s^{-4}$. The presence of these types of terms will show up clearly by comparing experiments done at Serpukhov, FNAL, and CERN ISR energies. Note also that the correction terms in the triple-Regge region given in Eq. (41) are the same terms that dominate the large-p_T region. Hence one should be able to normalize them in one region and test this aspect of the theory in the other kinematic domain. The above form for the inclusive cross section, with the ϵ dependences for H_1 and H_2 as predicted by dimensional counting, gives a good description of the inclusive data from $p_L \sim 25$ GeV/c to the CERN ISR range for $p_T \gtrsim 0.7$ GeV/c. The x_L dependence of the lower-energy data is also reasonably fit in the range $0 < x_L < 0.5$.

One property which is unique to the CIM is the prediction on the basis of quark counting that all "similar" processes should have approximately the same differential cross sections at fixed angle; for example, all meson-baryon cross sections should be of the same order of magnitude at 90°, that is,

$$d\sigma(\pi p \to \pi p) \approx d\sigma(\pi^+ p \to K^+ \Sigma^+)$$

$$\approx d\sigma(Kp \to Kp)$$

$$\approx d\sigma(\pi p \to \rho p)$$

$$\approx d\sigma(\pi p \to \pi^0 n)$$

$$\approx d\sigma(\bar{p}p \to \pi\pi)$$

$$\approx d\sigma(\bar{p}p \to \bar{K}K), \quad \text{etc.}$$

It therefore follows that the inclusive production of various mesons and the low mesonic resonance will all be of the same order of magnitude in pp collisions, away from the exclusive limit which is controlled by the threshold behavior of the $G(z)$ functions involved. The decay of resonances can provide an important source of lower-momentum pions as discussed by Bjorken and Farrar.[31]

In this paper a general treatment of the probability functions $G_{a/A}(z)$ was given based upon dimensional counting and the concept of reducible and irreducible graphs. The predicted properties of the G's can be tested experimentally by measuring the inclusive cross sections near their exclusive limit (including the fragmentation region), by measuring the particle ratios in the same region, and by measuring the single-particle-decay spectrum of very unstable systems (such as $B\bar{B}$ and e^+e^-). The important subprocesses which control large-p_T reactions can be further identified by measuring the associated multiplicities and the distribution of quantum numbers in the final states.

The structure of our formulas for inclusive cross sections has a simple physical basis and

interpretation. The leading power, N, of p_T^{-2} measures the minimum number of elementary fields that must be involved in the basis high-p_T subprocess. The leading power of ϵ, on the other hand, P, measures the "degree of forbiddeness" of the transition—that is, the amount of bremsstrahlung that must take place in order to produce the observed final particle via the given subprocess. These two powers are not independent in the CIM since they must satisfy the relation $N + P = n - 3$, where n is the minimum number of fields in the corresponding exclusive-limit channel. The system of counting rules provided by the CIM plus dimensional counting yields the simplest possible formulas which are consistent with the observed power laws and the constraints of continuity with low-p_T processes, exclusive processes, etc. The theory thus sets a pattern for the expected behavior of strong-interaction processes throughout the entire Peyrou plot, and predicts in a precise way that inclusive cross sections will depend critically on the quantum numbers of the detected particle and the beam particle.

One of the main virtues of the CIM is the large number of testable predictions that follow from its calculational rules. However, it should be stressed that the CIM is a model and its calculational rules were introduced such that they are both simple and definite, and in addition, are reasonable in terms of more familiar theories. These rules need to be derived from a more fundamental theory of hadronic matter which incorporates a mechanism for permanent quark binding. We assume that the very unusual property of the force that will not allow the constituents to escape will also explain the rule that constituents of different hadrons do not interact directly.[32]

This rule may be difficult to derive from a conventional standpoint. However, it is necessary empirically in order to remove possible "hard" vector-gluon exchanges from the theory which could predict a s^{-2} behavior at fixed x_T in the inclusive cross section. It was originally introduced to explain the differences in the behavior at large angles of the differential cross sections for pp and $\bar{p}p$, and also K^+p and K^-p at quite low energies. In any case, the constituent-interchange graphs must be present in any constituent theory. We assume that they dominate the amplitude and thereby achieve a model with considerable predictive power.

Recently Landshoff[33] has noted that in models which allow gluon exchange between hadrons, the multiple (Glauber) scattering of nearly-on-shell quarks will dominate hadron-hadron scattering processes at fixed angle. If gluon exchange between the quarks is scale-invariant, then this am-

plitude leads the dimensional-counting contributions by the power $(\sqrt{s}\,)^{N-1}$, where N is the number of on-shell quark scatterings. However, in the CIM, gluon exchange between quarks of different hadrons is not allowed, and these contributions do not arise. A very interesting argument has also been presented by Polkinghorne.[34] He notes that in neutral-vector-gluon–exchange models, higher-order graphs give an exponential factor $\exp[-\alpha \ln^2(s/\lambda^2)]$ which suppresses on-shell quark-quark scattering. However, the interchange graphs, since they involve off-shell wave functions, may still obey dimensional counting in this type of model.

In summary, the main physical predictions of the CIM basically arise from the power falloff of the hadronic wave functions.[35] In contrast to the typical exponential behavior of conventional Regge amplitudes, this allows us to continue simply from one Regge region to another, and to the region of large transverse momentum in both inclusive and exclusive processes. The CIM appears to reflect correctly the behavior of hadronic matter at short distances and its essential degrees of freedom. Further experimental tests are necessary in order to define precisely the limits of validity of the model.

ACKNOWLEDGMENTS

*Work supported by the U. S. Atomic Energy Commission.

[1] F. W. Büsser et al., Phys. Lett. 46B, 471 (1973); M. Banner et al., ibid. 44B, 537 (1973); B. Alper et al., ibid. 44B, 521 (1973).

[2] J. W. Cronin et al., Phys. Rev. Lett. 31, 1426 (1973).

[3] J. V. Allaby et al., CERN Report No. CERN-TH-70-11, 1970 (unpublished); E. W. Anderson et al., Phys. Rev. Lett. 19, 198 (1967).

[4] France–Soviet Union Collaboration, communication to the Aix-en-Provence International Conference on Elementary Particles, 1973 (unpublished). We wish to thank Dr. E. Pauli for interesting conversation on the large-P_T aspects of this data.

[5] R. Anderson et al., Phys. Rev. Lett. 30, 627 (1973).

[6] The fit to kaon data is also good. See G. W. Brandenburg et al., Phys. Lett. 44B, 305 (1973); A. Lundby, in High Energy Collisions—1973, proceedings of the fifth international conference, Stony Brook, 1973, edited by C. Quigg (A. I. P., New York, 1973); C. Baglin et al., Phys. Lett. 47B, 85 (1973); 47B, 98 (1973).

[7] S. M. Berman, J. D. Bjorken, and J. B. Kogut, Phys. Rev. D 4, 3388 (1971).

[8] J. F. Gunion, S. J. Brodsky, and R. Blankenbecler, Phys. Rev. D 6, 2652 (1972); Phys. Lett. 42B, 461 (1972). To help settle questions of covariance in the approach used above, see M. Schmidt, Phys. Rev. D 9, 408 (1974).

[9] J. F. Gunion, S. J. Brodsky, and R. Blankenbecler, Phys. Lett. 39B, 649 (1972); Phys. Rev. D 8, 287 (1973).

[10] P. V. Landshoff and J. C. Polkinghorne, Phys. Lett. 45B, 361 (1973); Phys. Rev. D 8, 927 (1973); 8, 4157 (1973).

[11] D. Horn and M. Moshe, Nucl. Phys. B48, 557 (1972); B57, 139 (1973); J. Kogut, G. Frye, and L. Susskind, Phys. Lett. 40B, 469 (1972); R. M. Barnett and D. Silverman, UCI report, 1973 (unpublished). See also W. R. Theis, Phys. Lett. 42B, 246 (1972).

[12] D. Amati, L. Caneschi, and M. Testa, Phys. Lett. 43B, 186 (1973); S. D. Ellis and M. B. Kislinger, Phys. Rev. D 9, 2027 (1974).

[13] J. M. Cornwall and D. J. Levy, Phys. Rev. D 3, 712 (1971).

[14] S. J. Brodsky and G. R. Farrar, Phys. Rev. Lett. 31, 1153 (1973); V. Matveev, R. Muradyan, and A. Tavkhelidze, Nuovo Cimento Lett. 7, 719 (1973). See also D. M. Scott, DAMTP Report No. 73/37 (unpublished); and Z. F. Ezawa, DAMTP Report No. 7415, 1974 (unpublished).

[15] This comment does not apply to the "soft" gluon models of H. M. Fried and T. K. Gaisser, Phys. Rev. D 7, 741 (1973); H. M. Fried, B. Kirby, and T. K. Gaisser, ibid. 8, 3210 (1973).

[16] J. D. Bjorken and J. Kogut, Phys. Rev. D 8, 1341 (1973); D. M. Scott, DAMTP Report No. 73/37 (unpublished).

[17] R. Blankenbecler, S. J. Brodsky, J. F. Gunion, and R. Savit, Phys. Rev. D 8, 4117 (1973); 10, 2153 (1974).

[18] S. D. Drell and T.-M. Yan, Phys. Rev. Lett. 24, 181 (1970); G. B. West, ibid. 24, 1206 (1970).

[19] E. D. Bloom and F. J. Gilman, Phys. Rev. Lett. 25, 1140 (1970).

[20] A. Mueller, Phys. Rev. D 2, 2693 (1970).

[21] G. R. Farrar, Nucl. Phys. B77, 429 (1974).

[22] J. G. Gunion, Phys. Rev. D 10, 242 (1974). In this paper, the interesting proposal is made that $g(d/p)$ (d =down quark) is one larger than $g(u/p)$ (u = up quark). This has interesting consequences for the ratio of the neutron and proton structure functions near $x=1$, the effective α's to be described shortly, and the π^+/π^- ratio in inclusive reactions.

[23] J. Tran Than Van, J. F. Gunion, D. Coon, and R. Blankenbecler, in preparation. For an alternative approach and predictions, see K. Kinoshita, Prog. Theor. Phys. 51, 1989 (1974).

[24] R. Pearson has shown that the above predictions are in good agreement with the pion charge-exchange data (private communication).

[25] S. D. Drell and T.-M. Yan, Phys. Rev. D 1, 1617 (1970).

[26]The idea that the decay of the $(N\bar{N})$ system should be related to the nucleon structure function was introduced and discussed by E. Pelaquier and F. M. Renard, contribution to the Ninth Rencontre de Moriond, Meribel, France, 1974 (unpublished). We thank Dr. Pelaquier for interesting discussions on their treatment of the data.

[27]R. P. Feynman, Phys. Rev. Lett. 23, 1415 (1969).

[28]Our approach generalizes the suggested threshold relation given by H. Goldberg, Nucl. Phys. B44, 149 (1972).

[29]Min-Shih Chen, Ling-Lie Wang, and T. F. Wong, Phys. Rev. D 5, 1667 (1972).

[30]G. Fox and R. D. Field, Caltech report, 1974 (unpublished), and references therein.

[31]J. D. Bjorken and G. R. Farrar, Phys. Rev. D 9, 1449 (1974).

[32]While this assumption may seem to be incomfortable to many readers, it should be pointed out that the vector-gluon enthusiasts usually compute only the gluon-exchange graphs and completely neglect the constituent-interchange graphs even in processes in which they are of the same order and fall in s at the same rate as the former at fixed angle.

[33]P. Landshoff, Phys. Rev. D 10, 1024 (1974).

[34]J. Polkinghorne, Phys. Lett. 49B, 277 (1974).

[35]The predicted behaviors cannot be derived from a general approach such as the Deser-Gilbert-Sudarshan (DGS) representation alone, as has been emphasized by P. M. Fishbane and I. J. Muzinich, Phys. Rev. D 8, 4015 (1973).